

Implementation of Retinal Pathways

Payal Shah, Satvik Sawant, Raviraj Randive, Shauryavir Singh Manhas and Surendra Singh Rathod

Cite as: Shah, P., Sawant, S., Randive, R., Singh Manhas, S., & Singh Rathod, S. (2023). Implementation of Retinal Pathways. International Journal of Microsystems and IoT, 1(7), 445–451. <https://doi.org/10.5281/zenodo.10441440>




© 2023 The Author(s). Published by Indian Society for VLSI Education, Ranchi, India



Published online: 18 December 2023.



Submit your article to this journal: 




Article views: 



View related articles: 



View Crossmark data: 

DOI: <https://doi.org/10.5281/zenodo.10441440>



Implementation of Retinal Pathways

Payal Shah¹, Satvik Sawant¹, Raviraj Randive¹, Shauryavir Singh Manhas¹ and Surendra Singh Rathod²

¹ Department of Electronics Engineering, Sardar Patel Institute of Technology, Mumbai, India

² Department of Electronics & Computer Science, Fr. Conceicao Rodrigues College of Engineering, Mumbai, India

ABSTRACT

Research in Retinal Pathways has been increasing in recent times. This research opens so many possibilities of analog computation techniques in future. To advance the research in this domain, understanding of mathematical formulation and electrical properties of retinal pathways is necessary. By analysing this formulation, a transistorized design of retinal pathways. Both the mathematical and transistorised model are implemented using MATLAB and LTspice respectively and it works for same input conditions and produces similar output. The transistorized design effectively produces the stimulus from rod and cone cells to ganglion cells..

KEYWORDS

retinal pathway, computational model, VLSI (PM)

1. INTRODUCTION

A retinal pathway is a pathway which is responsible for sending visual sensations from the retina to the brain.

The complex and subtle structures that form the retina are associated with almost equally complex mathematical models. The model is created with highlevel mathematical blocks, which allow a better understanding into circuit methodologies adaptable with top-down hardware mapping in order to ensure faster computing. In order to create a hardware compatible model, the fundamentals of a retinal pathway must be known. Neuronal nonlinearities and related complexities necessitate knowledge of neuroanatomical processes. The retinal circuitry processes the signals from the photoreceptors and converts them into a code of neural impulses when light impinges on the photoreceptors on the retina's surface.

In this study, a simulation platform for neural computing is present in the retina which is responsible for a collection of nonlinear ordinary differential systems being converted to integral system that can be adapted using a top-down VLSI architecture. Although these coupled differential equations are quite difficult to be solved using conventional methods. Software based tools like python are favoured over these convention techniques.

The research simulates neural signals using non-linear integral equations which are implemented on hardware. The mathematical efficiency needed by bio-systems is achieved by giving a mathematical method for answering integral equations. The first step is to create a framework for first-level bioflow model. The model is based on the biochemical reaction hypothesis which supports Hodgkin and Huxley model on ionic current gating theory through kinetic-driven quantitative modelling of the action potential.

The model that will arise through this experimentation would be expected to have increased efficiency.

Researchers are trying to make new chips based on these methodology. Chips having architecture as same as normal chips with slight modification on processing and encoding side were created. From these researches, none of the chips include the whole pathway flow. In this paper, a transistorised design of whole retinal pathway is created.

2. LITERATURE SURVEY

The survey is divided into 3 parts, Bioflow model of retinal pathways, mathematical modelling and implementation of transistorized circuit.

Studying bioflow modelling gives us the information about the exact structure of retinal pathways, the types of neurons present in the pathways, various electrochemical processes going on in the neurons. It also tells about the exact functioning of each neurons present in the pathways and how it contributes in the process of phototransduction and visual processing.

(Jason K. Eshraghian et al. 2016) has proposed the model for dual pathways.[1]

Their signal flow model includes total 6 neurons. The model started with the rod and cone cells which convert the light incident on the retina an electrical stimulus. The amacrine cells integrate the message received from the previous stage and pass it through to the ganglion cells. The message is passed via the bipolar cells which act as a pathway between the two. All of these neurons generate action/reduction potential. This potential propagates through further cells and finally passes from ganglion cells through optic nerve to the brain.[2]

The light acts as stimulus for various chemical reactions happening inside the photoreceptors and current generation[3]. The horizontal cell is present in between these stages and it acts as a feedback element between the two. The outcome of this stage is handed over to the bipolar cell.

There are two types of bipolar cell i. e. ON and OFF bipolar cell[4]. Depending upon the input conditions, either one of the cells get activated and passes the stimulus to the corresponding ganglion cell.

In retinal pathways there are total 4 ionic currents namely potassium current, Calcium Current, Calcium Activated chlorine current, calcium activated potassium current, hyperbolic current and leakage current in each cell. In photoreceptors, one additional current exits which is photo-current. The value of receptor potential changes when the current from the photoreceptor passes through the neuron. In other cells (like bipolar, amacrine, ganglion) the process is initiated because of synaptic current[5].

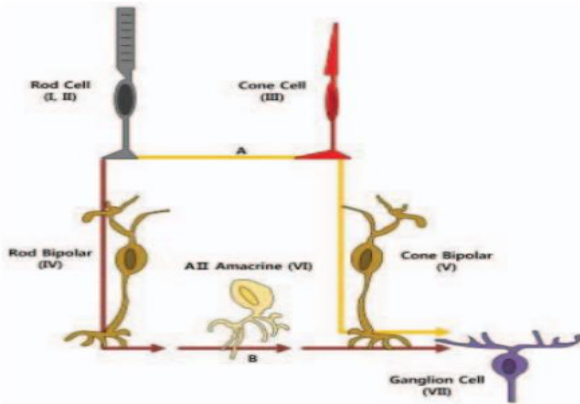


Fig. 1 Dual flow architecture of Retinal Pathways

(Kimihiro Nishio et al. 2004) proposed a CMOS biological vision system. The paper explained that the functions of edge and motion capturing was performed by the retina. The paper presented an edge capturing model using CMOS technology. The pathway to be chosen was decided on the basis of a threshold where if the input from the photodiode region was greater than the threshold, then the pathway for cones would be taken, else, the rod pathway would be chosen. This circuit could detect the edges for the photocurrent ranging between 1pA to 100nA. It also had a dynamic swing of 5 decibels [6]. The previous motion generating model utilized current mirror circuits, it faced issues in operation due to device mismatch. The model implemented here had the function to digitize the edge signals it obtained. This circuit was made using MOS switches instead of current mirror circuits so as to reduce the device mismatch.

3. STRUCTURE AND WORKING OF RETINAL PATHWAYS

3.1. Biological flow of Retinal Pathways:

First layer of retinal pathways consists of photoreceptors i.e. Rod cells and Cone cells. Particular type of cone cells are sensitive to all intensities of that type of wavelength because for different intensities photoreceptors produces different membrane potentials. For RGB light waves incident on retina, respective cone cells generate a membrane potential. For any color other than First layer of retinal pathways consists of photoreceptors i.e. Rod cells and Cone cells. Particular type of cone cells are sensitive to all intensities of that type of wavelength because for different intensities photoreceptors produces different membrane potentials. For RGB light waves incident on retina, respective cone cells generate a membrane potential. For any color other than RGB, cone cells generate membrane potential where value of membrane potential for each type of cell depends on the

incident wavelength. When light is incident, membrane potential suddenly drops to some value and again starts increasing steadily. Biologically, when light falls on photoreceptors, flow of sodium ions(cations) through photoreceptors decreases which in turn reduces the membrane potential. In absence of light, flow of sodium ion through photoreceptors increases which causes Depolarization of photoreceptors. During depolarization, more glutamate is released

Depending upon the overall glutamate released during hyperpolarization and depolarization of photoreceptors, Horizontal cells start their process of lateral inhibition. Biologically, its the process by which horizontal cells inhibits the flow of glutamate. If any group of photoreceptors releases less amount of glutamate the lateral inhibition is diminished. If any group of photoreceptors releases more glutamate then the lateral inhibition is enhanced. Due to this inhibition membrane potential at the end of photoreceptor start increasing from its lower value and reaches to its initial value. When mebrane potential reaches to its initial value, process of lateral inhibition stops and membrane potential remains in that value (which is -35mV) till light illuminates the retina again. RGB, cone cells generate membrane potential where value of membrane potential for each type of cell depends on the incident wavelength. When light is incident, membrane potential suddenly drops to some value and again starts increasing steadily. Biologically, when light falls on photoreceptors, flow of sodium ions(cations) through photoreceptors decreases which in turn reduces the membrane potential. In absence of light, flow of sodium ion through photoreceptors increases which causes Depolarization of photoreceptors. During depolarization, more glutamate is released.

Depending upon the overall glutamate released during hyperpolarization and depolarization of photoreceptors, Horizontal cells start their process of lateral inhibition. Biologically, its the process by which horizontal cells inhibits the flow of glutamate. If any group of photoreceptors releases less amount of glutamate the lateral inhibition is diminished.

If any group of photoreceptors releases more glutamate then the lateral inhibition is enhanced. Due to this inhibition membrane potential at the end of photoreceptor start increasing from its lower value and reaches to its initial value. When mebrane potential reaches to its initial value, process of lateral inhibition stops and membrane potential remains in that value (which is -35mV) till light illuminates the retina again.

This response of photoreceptors works as a stimulus for bipolar cells in second layer of retinal pathways. Bipolar cell amplifies the output of photoreceptors. There are two types of bipolar cells i. e. ON bipolar cells and OFF bipolar cells.

Graphically, lowering the membrane voltage of rod and cone cells causes lowering the membrane voltage of corresponding OFF Bipolar Cell and vice versa. In case of ON bipolar cell, lowering the membrane voltage of rod and cone cells increases the membrane potential of bipolar cell and vice versa. This process brings certain kind of selectivity which activates some cells and deactivates other cells.

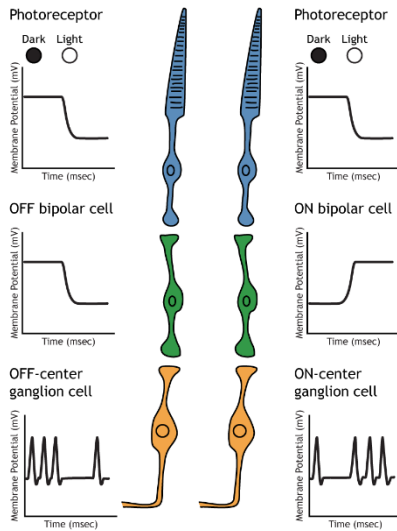


Fig. 2 Dual flow architecture of Retinal Pathways[7]

If we move a group of photoreceptors from dark condition to light, their membrane potential reduces (hyperpolarization). The voltage of the neural membrane is brought down for OFF bipolar cells. In other words, the OFF bipolar cell hyperpolarizes. When the same conditions are applied to the other type of cell, a contrasting effect is seen in them as they depolarize. Swapping the state of these cells will bring about a reversal in the spiking frequency.

In simple terms, ganglion cells act like pulse position modulator. Changes in the rate of spiking signals from ganglion cells are captured by brain to process the information.

3.2. Method used for Mathematical Modelling:

Before we dive into the circuit implementation part, we first need to understand the functionality of retinal pathways mathematically. Conductance-based neuronal models describe m and h with differential equations of identical form with voltage-dependent transition rates.

$$C_m \frac{dV}{dt} = \sum I_{ion}([V, \chi; [Ca^{2+}]]) + I_{syn}(V) \quad (1)$$

$$\frac{d[Ca^{2+}]}{dt} = I_{Ca}(V) + G(V; [Ca^{2+}]) \quad (2)$$

$$\frac{d\chi}{dt} = (1-\chi)\alpha_\chi(V) - \beta_\chi(V) \quad (3)$$

here, $\sum I_{ion}([V, \chi; [Ca^{2+}]])$ gives summation of all ionic currents and C_m will signify the capacitance of the membrane and the I_{syn} represents synaptic current input.

3.2.1. Method of Curve Fitting:

This method creates an equation in terms of standard mathematical expression which makes the computation simpler. The transduction process is not replicated here. I_{photo} is,

$$I_{photo}(t) = I_{dark}(t) + A(t) \left[\left(1 - e^{-t/\tau_1}\right) - \left(\frac{1}{1 + e^{-(t-b)/\tau_2}}\right) + \left(1 - e^{-t/\tau_3}\right) \right] \quad (4)$$

here, I_{dark} signifies the dark current which has a value of 40pA. τ_1 , τ_2 , τ_3 and b are constants and their values fall approximately at 50ms, 450ms, 800ms and 3800ms. $A(t)$ is a time varying step signal which represents the amplitude of I_{photo} [8].

4. MATHEMATICAL MODEL [1]

4.1. Membrane Potential:

$$I_{ALL} = I_{photo} + I_h + I_{Kv} + I_{Ca} + I_{Cl(Ca)} + I_{K(Ca)} \quad (5)$$

$$C_m \frac{dV}{dt} = -I_{ALL}(V(0) = -36.186), C_m = 0.02 [nF] \quad (6)$$

4.2. Rod Photocurrent:

$$\frac{dRh}{dt} = J_{hv} - \alpha_1 * Rh + \alpha_2 * Rh_i, Rh(0) = 0 \quad (7)$$

$$\frac{dRh_i}{dt} = \alpha_1 * Rh - (\alpha_2 + \alpha_3) * Rh_i, Rh(0) = 0 \quad (8)$$

$$\frac{dT_r}{dt} = \epsilon * Rh * (T_{tot} - T_r) - \beta_1 * T_r + \tau_2 * PDE - \tau_1 * T_r * (PDE_{tot} - PDE), T_r(0) = 0 \quad (9)$$

$$\frac{dPDE}{dt} = \tau_1 * T_r * (PDE_{tot} - PDE) - \tau_2 * PDE, (PDE(0) = 0) \quad (10)$$

$$\frac{d[Ca^{2+}]}{dt} = b * J - \gamma_{Ca} * ([Ca^{2+}] - Ca_0) - k_1 * (e_T - [Ca^{2+}]) * [Ca^{2+}] + k_2 * Cab \quad (11)$$

$$\frac{dCab}{dt} = k_1 * (e_T - [Cab]) * [Ca^{2+}] - k_2 * [Cab], ([Cab](0) = 34.88) \quad (12)$$

$$\frac{dcGMP}{dt} = \frac{A_{max}}{1.0 + ([Ca^{2+}]/Kc)^4} - cGMP * (\bar{V} + \alpha * PDE) \quad (13)$$

$$J = \frac{J_{max} * (cGMP)^3}{(cGMP^3 + 10^3)} \quad (14)$$

$$I_{photo} = -J * \left[1.0 - \exp\left(\frac{V-8.5}{17.0}\right) \right] \quad (15)$$

4.3. Hyperpolarization activated current:

$$\alpha_{hCa} = \frac{8}{\exp\left(\frac{V+78}{14}\right) - 1}, \quad (16)$$

$$\beta_{mCa} = \frac{18}{\exp\left(\frac{-V+8}{19}\right) + 1} \quad (17)$$

$$I_h = \bar{g} * (O_1 + O_2 + O_3) * (V - E_h), \bar{g} = 3.0 [nS], E_h = -32 [mV] \quad (18)$$

$$\frac{dC_1}{dt} = -4\alpha_h C_1 + \beta_h C_2 \quad (19)$$

$$\frac{dC_2}{dt} = 4\alpha_h C_1 - 3(\alpha_h + \beta_h) C_2 + \beta_h O_1 \quad (20)$$

$$\frac{dO_1}{dt} = 3\alpha_h C_2 - 2(\alpha_h + \beta_h) O_1 + 3\beta_h O_2 \quad (21)$$

$$\frac{dO_2}{dt} = 2\alpha_h O_1 - (\alpha_h + 3\beta_h) O_2 + 4\beta_h O_3 \quad (22)$$

$$\begin{aligned} \frac{dO_3}{dt} &= \alpha_h O_2 - 4\beta_h O_3 \\ C_1(0) &= 0.646, C_2(0) = 0.298, O_1(0) = 0.0517, \\ O_2(0) &= 0.00398, O_3(0) = 0.000115 \end{aligned} \quad (23)$$

4.4. Calcium Current:

$$\alpha_{m_{Ca}} = \frac{3(80-V)}{\exp\left(\frac{80-V}{25}\right) - 1} \quad (24)$$

$$\beta_{m_{Ca}} = \frac{10}{1 + \exp\left(\frac{V+38}{7}\right)} \quad (25)$$

$$h_{Ca} = \frac{\exp\left(\frac{40-V}{18}\right)}{1 + \exp\left(\frac{40-V}{18}\right)} \quad (26)$$

$$\frac{dm_{Ca}}{dt} = \alpha_{m_{Ca}} * (1 - m_{Ca}) - \beta_{m_{Ca}} * m_{Ca}, m_{Ca}(0) = 0.436 \quad (27)$$

$$I_{Ca} = \bar{g}_{Ca} - m_{Ca}^4 * h_{Ca} * (V - E_{Ca}) \quad (28)$$

$$\bar{g}_{Ca} = 0.7[\text{nS}], E_{Ca} = -12.5 \log\left(\frac{[Ca]_s}{[Ca]_0}\right), [Ca]_0 = 1600[\mu\text{M}] \quad (29)$$

4.5. Calcium activated Chloride current:

$$m_{Cl(Ca)} = \frac{1}{1 + \exp\left(\frac{0.37 - [Ca]_s}{0.09}\right)} \quad (30)$$

$$\begin{aligned} I_{Cl(Ca)} &= \bar{g}_{Ca(Cl)} - m_{Ca(Cl)} * (V - E_{Ca(Cl)}) \\ \bar{g}_{Ca(Cl)} &= 2.0[\text{nS}], -E_{Ca(Cl)} = -20[\text{mV}] \end{aligned} \quad (31)$$

4.6. Calcium activated Potassium current:

$$\alpha_{m_{K(Ca)}} = \frac{15(80-V)}{\exp\left(\frac{80-V}{40}\right) - 1} \quad (32)$$

$$\beta_{m_{K(Ca)}} = 20 \exp\left(\frac{-V}{35}\right) \quad (33)$$

$$\begin{aligned} \frac{dm_{K(Ca)}}{dt} &= \alpha_{m_{K(Ca)}} * (1 - m_{K(Ca)}) - \beta_{m_{K(Ca)}} * m_{K(Ca)} \\ &, m_{K(Ca)}(0) = 0.642 \end{aligned} \quad (34)$$

$$m_{K(Ca)} = \frac{[Ca]_s}{[Ca]_s + 0.3} \quad (35)$$

$$\begin{aligned} I_{K(Ca)} &= \bar{g}_{K(Ca)} * m_{K(Ca)}^2 * (V - E_k), \\ \bar{g}_{K(Ca)} &= 5.0[\text{nS}], E_k = -74[\text{mV}] \end{aligned} \quad (36)$$

4.7. Delayed Rectifier Current:

$$\alpha_{m_{Kv}} = \frac{5(100-V)}{\exp\left(\frac{100-V}{42}\right) - 1} \quad (37)$$

$$\beta_{m_{Kv}} = 9 \exp\left(-\frac{(V-20)}{40}\right) \quad (38)$$

$$\alpha_{h_{Kv}} = 0.15 \exp\left(-\frac{V}{22}\right) \quad (39)$$

$$\beta_{h_{Kv}} = \frac{0.4125}{\exp\left(\frac{10-V}{7}\right) + 1} \quad (40)$$

$$\begin{aligned} \frac{dm_{Kv}}{dt} &= \alpha * (1 - m_{Kv}) - \beta_{m_{Kv}} * m_{Kv} \\ &, m_{Kv}(0) = 0.430 \end{aligned} \quad (41)$$

$$\begin{aligned} \frac{dh_{Kv}}{dt} &= \alpha * (1 - h_{Kv}) - \beta_{h_{Kv}} * h_{Kv} \\ &, h_{Kv}(0) = 0.999 \end{aligned} \quad (42)$$

$$\begin{aligned} I_{Kv} &= \bar{g}_{Kv} * m_{Kv}^3 * (V - E_k) \\ &, \bar{g}_{Kv} = 2.0[\text{nS}], E_k = -74[\text{mV}] \end{aligned} \quad (43)$$

4.8. Leakage Current:

$$\begin{aligned} I_L &= g_L * (V - E_L) \\ &, g_L = 0.35[\text{nS}], E_L = -77[\text{mV}] \end{aligned} \quad (44)$$

5. SIMULATION RESULTS

5.1 V to I & I to V Converters

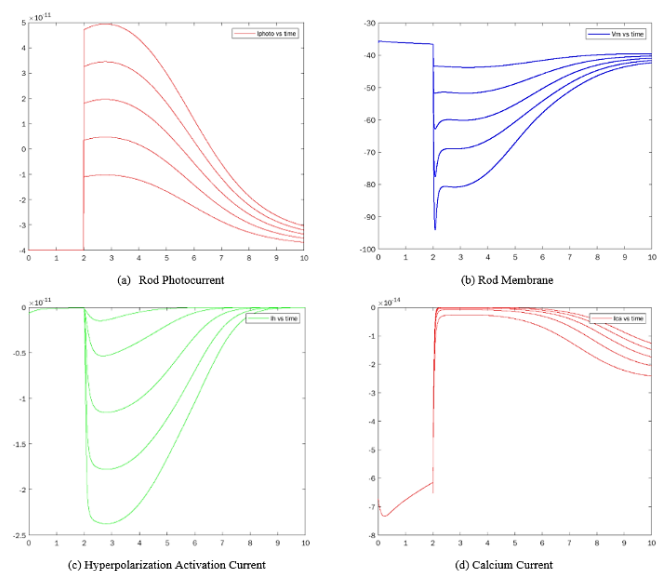


Fig. 3a Rod Photocurrent

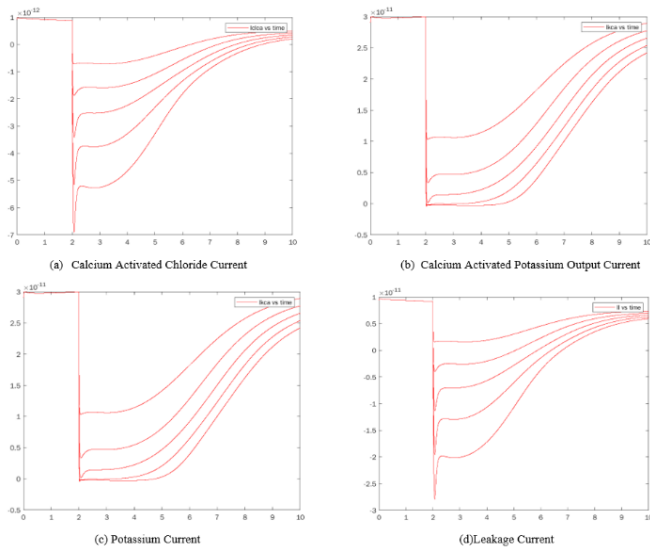


Fig. 3b Rod Photocurrent

5.2. Circuit Simulation Results:

Main aim of this project is to make a transistorised circuit which will produce similar response to that of the actual retinal pathways. As per the flow of mathematical model, when light is incident on photoreceptor, photo current is generated. It triggers the process of phototransduction and membrane potential varies as per the Fig. 4. Circuit in Fig. 5 represents the photoreceptor block.

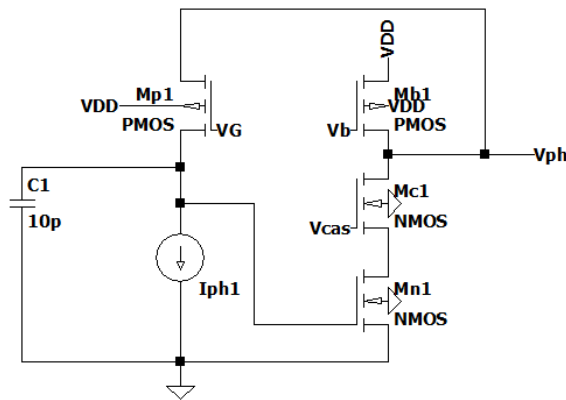


Fig. 4 Transistorized circuit of photoreceptor

Circuit in Fig. 4 is implemented and simulated on LTspice. The system functions in weak-inversion region and the value of Vph is given by

$$V_{ph} = V_G + nU_T \ln \left(\frac{I_{ph}}{I_{sp}} \right) \quad (45)$$

n signifies the weak-inversion slopefactor and Isp is the weak-inversion current factor for Mp1. Iph represents the photocurrent, which will give the corresponding variation in membrane potential [9].

However, because of the limitations of simulator used, we can't produce light inputs. Instead, we can imitate the required effects depending on the detection device used. Here, a current source is used to mimic the function of a photodetector. Current source is set to produce impulse signal.

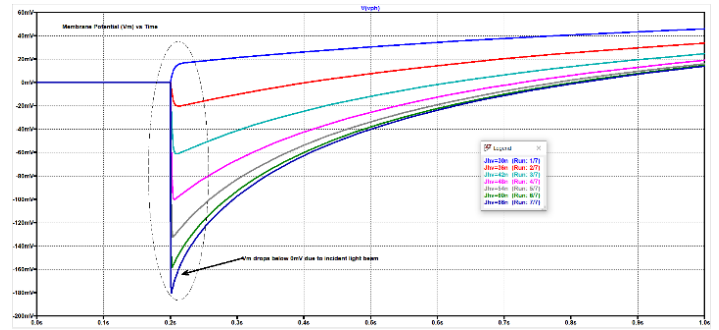


Fig. 5 Membrane potential plotted against time when light beam arrives at 200ms

In Fig. 5, variation of membrane potential is plotted against time for narrow spike of photocurrent at 200ms. The voltage falls below 0mV. After falling, it starts increasing and follows the results seen in Fig. 3a and Fig. 3b.

In Fig. 6, second block represents the preamplifier stage which amplifies the output of first block with positive phase shift. Preamplifier stage resembles the bipolar cells. NMOS numbered from 6-9 and 10-12 reside in weak-inversion.

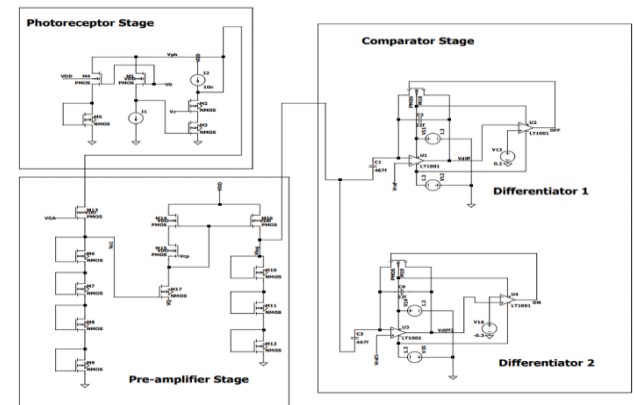


Fig. 6 Transistorized circuit of retinal pathways

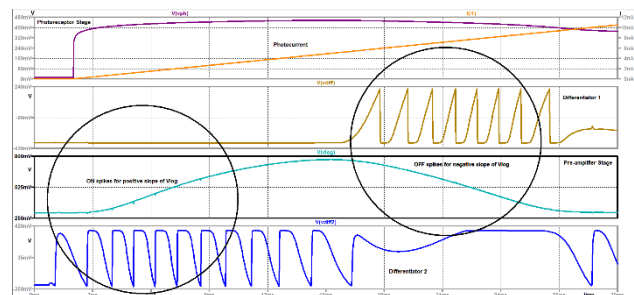


Fig. 7 Response for model of retinal pathways

These MOSFETS amplifies the output by the factor of n_n (slope factor) of MOSFETS in weak-inversion region. PMOS M14 to M16 forms current mirror. Further the signal is passed to 3rd stage which replicates the ganglion cells. It converts time varying bounded signals to spiking output. Third stage includes differentiators as well as comparators. Capacitors C2 and C4 charges and discharges continuously for positive and negative gradients of the output of preamplifier stage respectively. There are two parts of third stage. For positive gradient of output of preamplifier stage, one part produces spike (Differentiator 1). For negative gradient, other part produces spike (Differentiator 2). Another important feature of 3rd stage is that it produces pulse position modulated output depending

upon the gradient of preamplifier output.

Comparator compares whether the value of the output of differentiator is greater than the given value or lesser than the given value. Generally comparator has high output. In case of differentiator 1, if output of differentiator increases above the given value, comparator produces low output. The result is returned to the differentiator via PMOS which brings it back to its initial value. This process continues till the input of differentiator has non zero value (for differentiator 1) of slope. This is how positive spikes are produced for negative gradient of output of preamplifier. Similarly for positive gradient of output of preamplifier, same process continues in other way around producing negative spikes. Fig.7 depicts the results obtained for the 3rd stage.

6. CONCLUSION

The amount of exploration done on the Retinal Pathways is on the rise. The research presented helps provide a linkage between the mathematical conceptualization of the retinal properties and achieving a transistorized model for the same. The findings made here open the floor for various potential possibilities for analog computation in the future.

Retinal Pathways deals with special types of neurons present in the outer retina. These neurons carry different current components which are related to their membrane potential by transconductance which is similar to the behaviour of the MOSFETS. The ion channel gating variables of ion channels in retinal pathways are exponentially related to the membrane potential. The voltage response of given circuit matches the membrane potential of rod cells.

REFERENCES

1. J. K. Eshraghian (2016). Modelling and analysis of signal flow platform implementation into retinal cell pathway, 2016 IEEE Asia Pacific Conference on Circuits and Systems (APCCAS). <https://doi.org/10.1109/APCCAS.2016.7804011>
2. K. Cho (2016). Signal Flow Platform for Mapping and Simulation of Vertebrate Retina for Sensor Systems, in IEEE Sensors Journal, vol. 16, no. 15, pp. 5856-5866.. <https://doi.org/10.1109/JSEN.2016.2561310>
3. Forti S, Menini A, Rispoli G, Torre V. (1989). Kinetics of phototransduction in retinal rods of the newt Triturus cristatus. J Physiol. <https://doi.org/10.1113/jphysiol.1989.sp017873>
4. Boycott BB, Kolb H. (1973). The connections between bipolar cells and photoreceptors in the retina of the domestic cat. J Comp Neurol.. <https://doi.org/10.1002/cne.901480106>
5. Fohlmeister JF, Coleman PA, Miller RF. (1990). Modeling the repetitive firing of retinal ganglion cells. Brain Res. [https://doi.org/10.1016/0006-8993\(90\)91388-W](https://doi.org/10.1016/0006-8993(90)91388-W)
6. Yoshimi Kamiyama, Samuel M. Wu, Shiro Usui. (2009). Simulation analysis of bandpass filtering properties of a rod photoreceptor network, Vision Research, Volume 49, Issue 9.
7. Chapter 19 Vision: The Retina, Foundations of Neuroscience, <https://openbooks.lib.msu.edu/neuroscience/chapter/vision-the-retina/> [Accessed: August 23, 2021]
8. K. Nishio, K. Matsuzaka and N. Irie. (2004). Analog CMOS circuit implementation of motion detection with wide dynamic range based on vertebrate retina, IEEE Conference on Cybernetics and Intelligent Systems. <https://doi.org/10.1109/ICCIS.2004.1460687>
9. J. A. Leñero-Bardallo, T. Serrano-Gotarredona and B. Linares-Barranco. (2011). A 3.6 μ s Latency Asynchronous Frame-Free Event-Driven Dynamic-Vision-Sensor," in IEEE Journal of Solid-State Circuits, vol. 46, no. 6, pp. 1443-1455, <https://doi.org/10.1109/JSSC.2011.2118490>

AUTHORS



Payal Shah received her B. E. degree in Electrical Engineering in 2003 and M. E. degree with specialization in Automation Control and Robotics Engineering in 2005 from Maharaja Sayajirao University of Baroda, Vadodara, Gujarat. She worked as a Teaching Assistant at MS University from 2005 to 2006. Since 2006, she has been working as Lecturer and then an Assistant Professor at Sardar Patel Institute of Technology, Mumbai. In 2018, she joined the PhD program at Sardar Patel Institute of Technology, Mumbai. Her research interests include neuromorphic engineering, electronics devices and circuits, analog and mixed signal VLSI circuits.

Email: payal_shah@spit.ac.in



Satvik Sawant received his B.Tech. degree in Electronics Engineering in 2022 from Sardar Patel Institute of Technology, Mumbai Maharashtra. At present, he is working as developer in IT firm for data analysis and configuration. His special fields of interest include VLSI design, Artificial Intelligence, robotics, circuit simulation and Neuromorphic engineering.

Email: satvik.sawant@spit.ac.in



Raviraj Randive completed his B.Tech degree in Electronics Engineering from Sardar Patel Institute of Technology, Mumbai, in 2022. His special fields of interest are VLSI, digital electronics, deep learning and data science. Within his professional journey, He has been an integral part of an ML team lending his expertise to advance projects in OCR, object detection, LLMs.

Email: raviraj.randive@spit.ac.in



Shauryavir Manhas received his B.Tech degree in Electronics Engineering in 2022 from Sardar Patel Institute of Technology, Mumbai, Maharashtra. He has a keen interest in Artificial Intelligence, VLSI Design, Augmented Reality and Database Management. Since 2022, he is working as a developer in a finance firm helping them create and provide solutions to their clients.

Email: shauryavirsingh.manhas@spit.ac.in



Surendra Rathod received his B.E. degree in Electronics and Communications Engineering from Amravati University in 1997, M.E. degree in Electronics Engineering from VJTI, Mumbai in 2005 and PhD in Semiconductor Devices and VLSI Technology from IIT Roorkee in 2011. He is a professor of Electronics Engineering with more than 24 years of teaching experience. At present, he is working as the Principal at Fr. Conceicao

Rodrigues College of Engineering, Mumbai. His special fields of interest include VLSI design, Device modeling, Circuit simulation and Neuromorphic engineering. S. S. Rathod has acted as reviewer for various conferences and journals.

Email: ssrathodsir@gmail.com